

Quantum correlations and entanglement in coupled optomechanical resonators with photon hopping via Gaussian interferometric power analysis

Y. Lahlou, B. Maroufi, and M. Daoud

Citation: Chin. Phys. B, 2024, 33 (**5**): 050303. DOI: 10.1088/1674-1056/ad2a6e
Journal homepage: http://cpb.iphy.ac.cn; http://iopscience.iop.org/cpb

What follows is a list of articles you may be interested in

Enhancing quantum temporal steering via frequency modulation

Mengkai Wu(吴孟凯) and Weiwen Cheng(程维文)
Chin. Phys. B, 2024, 33 (**5**): 050306. DOI: 10.1088/1674-1056/ad2505

Complementary monogamy and polygamy properties among multipartite systems

Tao Li(李陶), Jing-Yi Zhou(周静怡), Qi Sun(孙琪), Zhi-Xiang Jin(靳志祥), Deng-Feng Liang(梁登峰), and Ting Luo(罗婷)
Chin. Phys. B, 2024, 33 (**3**): 030305. DOI: 10.1088/1674-1056/ad1748

Visualizing and witnessing first-order coherence, Bell nonlocality and purity by using a quantum steering ellipsoid in the non-inertial frame

Huan Yang(杨欢), Ling-Ling Xing(邢玲玲), Ming-Ming Du(杜明明), Min Kong(孔敏), Gang Zhang(张刚), and Liu Ye(叶柳)
Chin. Phys. B, 2023, 32 (**10**): 100305. DOI: 10.1088/1674-1056/acb762

Quantum steerability of two qubits mediated by one-dimensional plasmonic waveguides

Ye-Qi Zhang(张业奇), Xiao-Ting Ding(丁潇婷), Jiao Sun(孙娇), and Tian-Hu Wang(王天虎)
Chin. Phys. B, 2022, 31 (**12**): 120305. DOI: 10.1088/1674-1056/ac8af8

Coherence migration in high-dimensional bipartite systems

Zhi-Yong Ding(丁智勇), Pan-Feng Zhou(周攀峰), Xiao-Gang Fan(范小刚),Cheng-Cheng Liu(刘程程), Juan He(何娟), and Liu Ye(叶柳)
Chin. Phys. B, 2022, 31 (**6**): 060308. DOI: 10.1088/1674-1056/ac48f8

Quantum correlations and entanglement in coupled optomechanical resonators with photon hopping via Gaussian interferometric power analysis

Y. Lahlou[1,†], B. Maroufi[2], and M. Daoud[2]

[1] *LPHE-MS, Department of Physics, Faculty of Sciences, Mohammed V University, Rabat, Morocco*
[2] *LPMS, Department of Physics, Faculty of Sciences, Ibn Tofail University, Kénitra, Morocco*

(Received 1 December 2023; revised manuscript received 23 January 2024; accepted manuscript online 19 February 2024)

Quantum correlations that surpass entanglement are of great importance in the realms of quantum information processing and quantum computation. Essentially, for quantum systems prepared in pure states, it is difficult to differentiate between quantum entanglement and quantum correlation. Nonetheless, this indistinguishability is no longer holds for mixed states. To contribute to a better understanding of this differentiation, we have explored a simple model for both generating and measuring these quantum correlations. Our study concerns two macroscopic mechanical resonators placed in separate Fabry–Pérot cavities, coupled through the photon hopping process. this system offers a comprehensively way to investigate and quantify quantum correlations beyond entanglement between these mechanical modes. The key ingredient in analyzing quantum correlation in this system is the global covariance matrix. It forms the basis for computing two essential metrics: the logarithmic negativity ($E_{\mathcal{N}}^{\mathrm{m}}$) and the Gaussian interferometric power ($\mathcal{P}_{\mathcal{G}}^{m}$). These metrics provide the tools to measure the degree of quantum entanglement and quantum correlations, respectively. Our study reveals that the Gaussian interferometric power ($\mathcal{P}_{\mathcal{G}}^{m}$) proves to be a more suitable metric for characterizing quantum correlations among the mechanical modes in an optomechanical quantum system, particularly in scenarios featuring resilient photon hopping.

Keywords: quantum correlations, entanglement, Gaussian interferometric power, logarithmic negativity, optomechanics, photon hopping

PACS: 03.65.–w, 03.65.Ud, 03.67.–a, 42.50.–p **DOI:** 10.1088/1674-1056/ad2a6e

1. Introduction

Quantum correlations, as explored in numerous works,[1–4] occupy a central role in the landscape of quantum information theory,[5] propelling advancements in the realm of quantum technology.[6] Their significance extends across a spectrum of domains, encompassing quantum communication, quantum computing,[7–9] quantum cryptography,[10–12] and quantum metrology.[13–16] In light of this profound relevance, the study of quantum correlations has emerged as a captivating research domain within quantum information theory, encompassing both theoretical and experimental explorations. Notably, dedicated efforts are underway to generate these nonclassical correlations and ascertain optimal approaches for their manipulation and utilization as valuable resources for innovative information processing protocols.

Quantum entanglement, a particular form of quantum correlation, has garnered extensive investigation across diverse quantum systems.[17–20] It offers a profound insight into the foundational structure of quantum mechanics, serving as the principal demarcation between macroscopic (classical) and microscopic (quantum) systems.[21–23] Moreover, quantum entanglement has evolved into an indispensable asset in the realm of quantum information processing, where it underpins the remarkable computational speed of quantum computing and the unequivocal security of quantum communication. The latter relies on the availability of quantum entanglement.[24–26] As a result, the generation of quantum entanglement stands as a pivotal pursuit within the sphere of quantum information processing. This enthralling characteristic of the microscopic and subatomic domains[19] ushers forth a myriad of potential applications. These encompass quantum teleportation with fidelity surpassing classical cloning limits,[27] dense quantum coding, and even the detection of gravitational waves.[28] Furthermore, the study of quantum entanglement in macroscopic systems holds significant import, with various schemes put forward. These encompass the creation of entanglement between mirrors,[29] atomic ions,[30] and Cooper pairs.[31] Notably, it has been demonstrated that macroscopic entanglement can be generated through the influence of radiation pressure in optomechanical systems.

Optomechanical cavities[32–34] have emerged as a prevalent avenue for the investigation of quantum entanglement in macroscopic systems, with the introduction of diverse proposed protocols. These protocols hinge on the innate interaction between light and mechanical oscillators, offering a variety of avenues for creating quantum entanglement. Prominent among these methods are those enabling the generation of entanglement between vibrating mirrors,[35,36] atomic ions,[37] and entanglement across two separate cavities linked by an op-

†Corresponding author. E-mail: youness_lahlou@um5.ac.ma
© 2024 Chinese Physical Society and IOP Publishing Ltd

tical fiber.[38,39] In this manner, optomechanical cavities provide a foundational framework for establishing correlations among mechanical resonators,[29,40–44] leveraging the interplay between mechanical and optical degrees of freedom. This pivotal characteristic of optomechanical systems has spurred the exploration of macroscopic mechanical entanglement in a dual-cavity system.[29,45–47] In line with this perspective, our paper is centered on the examination of quantum correlations and the generation of quantum entanglement between mechanical resonators within a double optomechanical cavity system.

This study delves into generating macroscopic quantum entanglement within a dual-cavity optomechanical system. Our proposed methodology involves interconnecting two optomechanical cavities through photon hopping. In each cavity, a movable mirror at one end couples with a fixed mirror at the other, facilitating the interaction between the laser field and mechanical modes via photon hopping. This intricate coupling process culminates in the creation of quantum entanglement between the two mechanical modes. Consequently, we conduct a comprehensive examination of this generated quantum entanglement, extending our analysis to quantify a broader spectrum of quantum correlations that go beyond quantum entanglement. The primary objective of this study is to juxtapose the extent of quantum correlations with that of quantum entanglement within the established model. Our paper is structured as follows: In Section 2, we introduce the model encompassing two optomechanical cavities interconnected by photon hopping and submitted to a laser field. We present the Hamiltonian that governs the system's evolution and derive the quantum Langevin equations within the rotating wave approximation. Subsequently, we employ the linearization technique to acquire a set of coupled differential equations for the fluctuation operators, which are later resolved in the steady state. In Section 3, we give the system's covariance matrix describing the Gaussian state and the logarithmic negativity ($E_{\mathcal{N}}^{\mathrm{m}}$) and the Gaussian interferometric power ($\mathcal{P}_{\mathcal{G}}^{m}$) to quantify the extent of quantum entanglement and quantum correlations beyond entanglement between the two distinct mechanical modes. Section 4 is dedicated to a discussion of our findings, culminating in a concise summary of our work.

2. Model and Hamiltonian

The schema depicted above illustrates a quantum measurement[48] of an optomechanical cavity system, comprising two identical Fabry–Pérot cavities (as seen in Fig. 1). Each cavity features a fully reflecting mobile mirror, while the second one is a fixed mirror with partial transmissivity. Both cavities are simultaneously driven by a coherent laser field, with photon-hopping interactions facilitating the coupling of cavity fields. As a result, each cavity field interacts with the mechanical motion of the mechanical resonator through the effects of photon hopping. Each cavity's field is considered as a single-mode field with a frequency denoted as ω_{c_j}, where $(j=1,2)$. The pump laser's amplitude is determined as $|E_j|=\sqrt{\frac{2P_j\kappa_j}{\hbar\omega_{\mathrm{L}_j}}}$, with κ_j representing the energy decay rate of the two cavities, P_j signifying the laser's driving pump power, and ω_{L_j} representing the frequency of the vibrational modes. Additionally, the coupling coefficient between the cavity field and the movable mirror is defined as $g_j=(\omega_{\mathrm{c}_j}/L_j)\sqrt{\frac{\hbar}{m_j\omega_{m_j}}}$, where m_j signifies the mass of the mechanical mode, ω_{m_j} denotes the frequency of the mechanical oscillator, and L_j represents the length of each cavity.

The system's Hamiltonian can be expressed as (assuming $\hbar=1$)[35]

$$\hat{H}=\sum_{j=1,2}[(\omega_{\mathrm{c}_j}-\omega_{\mathrm{L}_j})a_j^{\dagger}a_j+\omega_{m_j}b_j^{\dagger}b_j+g_ja_j^{\dagger}a_j(b_j^{\dagger}+b_j)+\mathrm{i}(E_ja_j^{\dagger}\mathrm{e}^{-\mathrm{i}\omega_{\mathrm{L}_j}t}-E_j^{*}a_j\mathrm{e}^{\mathrm{i}\omega_{\mathrm{L}_j}t})]-\xi(a_1^{\dagger}a_2+a_2^{\dagger}a_1), \quad (1)$$

where a_j and b_j, as well as their respective Hermitian conjugates, denote the field operators associated with the two cavities and the two mechanical resonators (pertaining to the j^{th} optical mode and the j^{th} mechanical mode), characterized by resonant frequencies ω_{C} and ω_L. For the sake of simplicity, we assume $\omega_{\mathrm{L}1}=\omega_{\mathrm{L}2}$. The final term in the Hamiltonian accounts for the photon-hopping coupling between the two cavity modes, with a coupling strength represented as ξ. In the subsequent sections, our focus on the system's dynamics, which can be delineated through the quantum Heisenberg–Langevin (HL) equations in the Heisenberg representation.

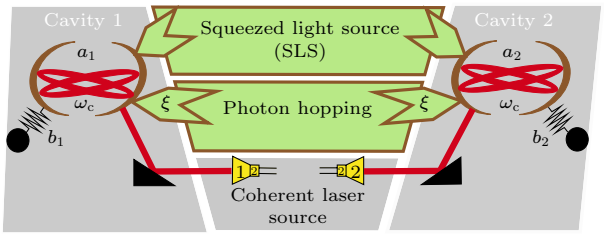


Fig. 1. Schematic of an optomechanical system composed of two separate optomechanical cavities, with each cavity featuring a fixed mirror in the middle and a movable mirror on the outside. These cavities are coupled to a two-mode squeezed light generated by spontaneous parametric down-conversion (SPDC) and connected via a photon hopping process (PH) with a coupling strength ξ. Each cavity is pumped by a coherent laser source with power P and frequency ω_{L}, characterized by an amplitude E_j.

2.1. Heisenberg–Langevin equation

The nonlinear HL equations of motion for the optical and mechanical modes, established in the rotating frame at the laser frequency, are simultaneously derived as[35]

$$\dot{a}_j=-\left(\frac{\kappa_j}{2}-\mathrm{i}\Delta_j\right)a_j-\mathrm{i}g_ja_j(b_j^{+}+b_j)+E_j+\mathrm{i}\xi a_k+\sqrt{\kappa_j}F_j^{\mathrm{in}}, \quad (2)$$

$$\dot{b}_j=-\left(\mathrm{i}\omega_m+\frac{\gamma_j}{2}\right)b_j-\mathrm{i}g_ja_j^{+}a_j+\sqrt{\gamma_j}f_j^{\mathrm{in}}, \quad (3)$$

where κ_j corresponds to the total decay rate of the cavity mode, while γ_j designates the damping rate of the mechanical mode. $\Delta_j = \omega_{\mathrm{L}_j} - \omega_{\mathrm{c}_j}$ denotes the laser detuning, f_j^{in} is the noise operator linked to the Brownian motion of the j^{th} movable mirror, and F_j^{in} represents the j^{th} input squeezed vacuum noise operator. These noise operators exhibit non-zero frequency-domain correlation functions, as elaborated in Refs. [49,50]:

$$\langle F_j^{\mathrm{in}\dagger}(t)F_j^{\mathrm{in}}(t')\rangle = \mathcal{N}\delta(t-t'), \tag{4}$$

$$\langle F_j^{\mathrm{in}}(t)F_j^{\mathrm{in}\dagger}(t')\rangle = (\mathcal{N}+1)\delta(t-t'), \tag{5}$$

$$\langle F_1^{\mathrm{in}}(t)F_2^{\mathrm{in}}(t')\rangle = \mathcal{M}\,\mathrm{e}^{-\mathrm{i}\psi}\delta(t-t'), \tag{6}$$

$$\langle F_1^{\mathrm{in}\dagger}(t)F_2^{\mathrm{in}\dagger}(t')\rangle = \mathcal{M}\,\mathrm{e}^{\mathrm{i}\psi}\delta(t-t'), \tag{7}$$

in this context, we define $\mathcal{N} = \sinh^2 r$, $\mathcal{M} = \sinh r\cosh r$, and $\psi = \omega_M(t+t')$, where r represents the squeeze parameter characterizing the squeezed light. It is worth noting that we make the assumption that the mechanical baths exhibit Markovian behavior, where the mechanical oscillator frequency ω_μ surpasses the damping rate γ. These baths manifest non-zero correlation properties between their noise operators, a subject elucidated in Refs. [51,52]:

$$\langle f_j^{\mathrm{in}\dagger}(t)f_j^{\mathrm{in}}(t')\rangle = n_{\mathrm{th}}\delta(t-t'), \tag{8}$$

$$\langle f_j^{\mathrm{in}}(t)f_j^{\mathrm{in}\dagger}(t')\rangle = (n_{\mathrm{th}}+1)\delta(t-t'), \tag{9}$$

here, we denote $n_{\mathrm{th}} = (\mathrm{e}^{\hbar\omega_\mu/k_{\mathrm{B}}T}-1)^{-1}$ as the average number of thermal phonons at the frequency of the mechanical resonator j, where k_{B} represents the Boltzmann constant and T signifies the temperature of the surrounding environment.

2.1.1. Classical dynamics

Solving analytically the coupled nonlinear quantum Langevin equations (2) and (3) is a challenging endeavor.[53] To obtain an analytical solution for these equations within the proposed model, we employ the following decomposition, in which the mode operators are represented as the sum of the mean in the steady state and a quantum fluctuation operator,

$$\delta b_j = b_j - \beta_j, \quad \delta a_j = a_j - \alpha_j, \tag{10}$$

with β_j and α_j denoting the steady-state average values for the mechanical and optical operators, respectively. The solutions of Eqs. (2) and (3) in the steady-state give explicit expressions for the mean values β_j and α_j as

$$\beta_j \equiv \langle b_j\rangle \equiv \frac{\mathrm{i}g_j|\alpha_j^{\mathrm{s}}|^2}{\frac{\gamma_j}{2}+\mathrm{i}\omega_m}, \tag{11}$$

$$\alpha_j \equiv \langle a_j\rangle \equiv \frac{\mathrm{i}\xi\alpha_k^{\mathrm{s}}+E_j}{\frac{\kappa_j}{2}-\mathrm{i}\Delta'_j}, \tag{12}$$

where we define $\Delta'_j = \Delta_j - g_j(\beta_j^* + \beta_j)$ as the effective detuning, which takes into account the displacement of the mirrors caused by photon hopping.

2.1.2. Linearization of quantum Langevin equations

Now, we examine the quantum statistical characteristics of the system by considering slight fluctuations of the operators around the steady-state classical mean values, as detailed in Eqs. (11) and (12). To this end, we introduce the substitutions $\delta b_j = b_j - \beta_j$ and $\delta a_j = a_j - \alpha_j$ into Eqs. (2) and (3), with the omission of the nonlinear terms $\delta a_j\delta a_j^\dagger$ and $\delta b_j\delta a_j$. This simplification is justified under the assumption that the mean values significantly surpass the variations. Consequently, the resulting Eqs. (2) and (3) can be expressed as

$$\begin{aligned}\delta\dot{a}_j = &-\left(\frac{\kappa_j}{2}-\mathrm{i}\Delta'_j\right)\delta a_j + G_j\left(\delta b_j^+ + \delta b_j\right) + \mathrm{i}\xi\,\delta a_k \\ &+\sqrt{\kappa_j}F_j^{\mathrm{in}},\end{aligned} \tag{13}$$

$$\delta\dot{b}_j = -\left(\mathrm{i}\omega_m + \frac{\gamma_j}{2}\right)\delta b_j + G_j\left(\delta a_j - \delta a_j^+\right) + \sqrt{\gamma_j}f_j^{\mathrm{in}}, \tag{14}$$

where $G_j = g_j|\alpha_j|$ signifies the multi-photon optomechanical coupling, and we define $\alpha_j = -\mathrm{i}|\alpha_j|$. In this study, we adopt the assumption that the system operates within the framework of the rotating wave approximation (i.e., $\Delta'_j = \omega_m$). This approximation corresponds to the regime of quantum state transfer, where one can safely neglect terms oscillating at $\pm 2\omega_m$. Utilizing the interaction picture for each operator O, defined as $\tilde{O}(\omega_m) = O\exp(\mathrm{i}\omega_m t)$, we derive the following expressions:

$$\delta\dot{\tilde{a}}_j = -\frac{\kappa_j}{2}\delta\tilde{a}_j + G_j\delta\tilde{b}_j^+ + \mathrm{i}\xi\,\delta\tilde{a}_k + \sqrt{\kappa_j}\tilde{F}_j^{\mathrm{in}}, \tag{15}$$

$$\delta\dot{\tilde{b}}_j = -\frac{\gamma_j}{2}\delta\tilde{b}_j - G_j\delta\tilde{a}_j^+ + \sqrt{\gamma_j}\tilde{f}_j^{\mathrm{in}}. \tag{16}$$

Hence, this linear differential system can be resolved through the application of Fourier transformation, following the lines presented in Ref. [54].

2.2. Covariance matrix

Following the linearization method of quantum Langevin equations, outlined in Ref. [44], we proceed to compute the elements of the covariance matrix which describe the Gaussian stationary states of the system.[44] For this end, we assume the presence of two identical cavities driven by identical laser sources and subjected to identical thermal baths.[44] Our objective is to deduce the explicit formula for the covariance matrix that characterizes the entire system. In this pursuit, we incorporate the following quadrature operators, which correspond to EPR-type quadrature operators for both mechanical and optical modes:[41]

$$\delta\tilde{X}^{\mathrm{m}_j}(t) = \frac{\delta\tilde{b}_j^\dagger + \delta\tilde{b}_j}{\sqrt{2}}, \quad \delta\tilde{Y}^{\mathrm{m}_j}(t) = \mathrm{i}\frac{\delta\tilde{b}_j^\dagger - \delta\tilde{b}_j}{\sqrt{2}}; \quad j = 1,2, \tag{17}$$

$$\delta\tilde{X}^{\mathrm{o}_j}(t) = \frac{\delta\tilde{a}_j^\dagger + \delta\tilde{a}_j}{\sqrt{2}}, \quad \delta\tilde{Y}^{\mathrm{o}_j}(t) = \mathrm{i}\frac{\delta\tilde{a}_j^\dagger - \delta\tilde{a}_j}{\sqrt{2}}; \quad j = 1,2. \tag{18}$$

Likewise, the Hermitian input quadrature noise is defined as

$$\tilde{X}^{\rm in}_{{\rm m}_j}(t)=\frac{\tilde{f}^{\rm in\dagger}_j+\tilde{f}^{\rm in}_j}{\sqrt{2}},\ \tilde{Y}^{\rm in}_{{\rm m}_j}(t)=\mathrm{i}\frac{\tilde{f}^{\rm in\dagger}_j-\tilde{f}^{\rm in}_j}{\sqrt{2}};\ j=1,2, \quad (19)$$

$$\tilde{X}^{\rm in}_{{\rm o}_j}(t)=\frac{\tilde{F}^{\rm in\dagger}_j+\tilde{F}^{\rm in}_j}{\sqrt{2}},\ \tilde{Y}^{\rm in}_{{\rm o}_j}(t)=\mathrm{i}\frac{\tilde{F}^{\rm in\dagger}_j-\tilde{F}^{\rm in}_j}{\sqrt{2}};\ j=1,2. \quad (20)$$

Indeed, the linearization of quantum Langevin equations illustrates that within each optomechanical cavity, the mechanical mode exhibits coupling to the quadrature fluctuations through the effective coupling $G_j=g|\alpha_j|$. This coupling becomes particularly pronounced as the amplitude $|\alpha_j|$ between the cavities increases. Additionally, the two cavity modes interact through photon hopping, characterized by a coupling strength ξ, which can be tailored to redistribute entanglement across distinct bipartite systems and induce entanglement between the mechanical modes.

In the realm of continuous variable systems, the utilization of phase space analysis is well-suited, requiring the adoption of the covariance matrix formalism[55,56] built upon quadrature operators. Consequently, we introduce an eight-component vector as follows:

$$u(t)=(\delta\tilde{X}^{\rm m_1}(t),\delta\tilde{Y}^{\rm m_1}(t),\delta\tilde{X}^{\rm m_2}(t),\delta\tilde{Y}^{\rm m_2}(t),\delta\tilde{X}^{\rm o_1}(t),\delta\tilde{Y}^{\rm o_1}(t),\delta\tilde{X}^{\rm o_2}(t),\delta\tilde{Y}^{\rm o_2}(t))^{\rm T},$$

where the notation $(O)^{\rm T}$ represents the transpose of an arbitrary operator O. The linearization of quantum Langevin equations can be expressed in the compact matrix form (Ref. [57])

$$\dot{u}(t)=Wu(t)+\eta(t), \quad (21)$$

where the term W represents the drift matrix. It is given by

$$W=\begin{pmatrix}\frac{-\gamma}{2}&0&0&0&-G&0&0&0\\0&\frac{-\gamma}{2}&0&0&0&G&0&0\\0&0&\frac{-\gamma}{2}&0&0&0&-G&0\\0&0&0&\frac{-\gamma}{2}&0&0&0&G\\G&0&0&0&\frac{-\kappa}{2}&0&0&-\xi\\0&-G&0&0&0&\frac{-\kappa}{2}&\xi&0\\0&0&G&0&0&-\xi&\frac{-\kappa}{2}&0\\0&0&0&-G&\xi&0&0&\frac{-\kappa}{2}\end{pmatrix}. \quad (22)$$

Furthermore, $\eta(t)$ corresponds to the noise vector and is defined as

$$\eta(t)=(\tilde{X}^{\rm in}_{\rm m_1}(t),\tilde{Y}^{\rm in}_{\rm m_1}(t),\tilde{X}^{\rm in}_{\rm m_2}(t),\tilde{Y}^{\rm in}_{\rm m_2}(t),\tilde{X}^{\rm in}_{\rm o_1}(t),\tilde{Y}^{\rm in}_{\rm o_1}(t),\tilde{X}^{\rm in}_{\rm o_2}(t),\tilde{Y}^{\rm in}_{\rm o_2}(t))^{\rm T}.$$

Hence, the covariance matrix can be obtained by solving the linearized Lyapunov equation, a process elucidated in Refs. [35,58],

$$W\Upsilon+\Upsilon W^{\rm T}-R=0, \quad (23)$$

with R denoting the diffusion matrix, which can be expressed as $R_{ij}\delta(t+t')=\frac{1}{2}(\langle\eta_i(t)\eta_j(t')+\eta_j(t')\eta_i(t)\rangle)$.

$$R=\begin{pmatrix}\gamma'&0&0&0&0&0&0&0\\0&\gamma'&0&0&0&0&0&0\\0&0&\gamma'&0&0&0&0&0\\0&0&0&\gamma'&0&0&0&0\\0&0&0&0&\kappa'&\mathcal{M}\kappa&0&0\\0&0&0&0&\mathcal{M}\kappa&\kappa'&0&0\\0&0&0&0&0&0&\kappa'&-\mathcal{M}\kappa\\0&0&0&0&0&0&-\mathcal{M}\kappa&\kappa'\end{pmatrix}, \quad (24)$$

in terms of the parameters $\gamma'=\gamma(n_{\rm th}+\frac{1}{2})$ and $\kappa'=\kappa(\mathcal{N}+\frac{1}{2})$. Subsequent to simple calculations employing the solution of Eq. (23), we obtain the following explicit expression for the quantum covariance matrix:

$$\Upsilon=[\Upsilon_{ij}]_{8\times8}=\begin{pmatrix}\Upsilon_{m_{1(2\times2)}}&\Upsilon_{m_{12(2\times2)}}&\Upsilon_{m_1o_{1(2\times2)}}&\Upsilon_{m_1o_{2(2\times2)}}\\\Upsilon^{\rm T}_{m_{12(2\times2)}}&\Upsilon_{m_{2(2\times2)}}&\Upsilon_{m_2o_{1(2\times2)}}&\Upsilon_{m_2o_{2(2\times2)}}\\\Upsilon^{\rm T}_{m_1o_{1(2\times2)}}&\Upsilon^{\rm T}_{m_2o_{1(2\times2)}}&\Upsilon_{o_{1(2\times2)}}&\Upsilon_{o_{12(2\times2)}}\\\Upsilon^{\rm T}_{m_1o_{2(2\times2)}}&\Upsilon^{\rm T}_{m_2o_{2(2\times2)}}&\Upsilon^{\rm T}_{o_{12(2\times2)}}&\Upsilon_{o_{2(2\times2)}}\end{pmatrix}. \quad (25)$$

To get the degree of pairwise quantum correlations between distinct modes, it is necessary to break down the covariance matrix into block matrices, with each sub-matrix of size 4×4. This decomposition results in a reduced covariance matrix, as represented by Eq. (25), in the following format

$$\Upsilon_{8\times8}=\begin{pmatrix}(\Upsilon_m)_{4\times4}&(\Upsilon_{mo})_{4\times4}\\(\Upsilon_{mo})^{\rm T}_{4\times4}&(\Upsilon_o)_{4\times4}\end{pmatrix}, \quad (26)$$

in this context, $(\Upsilon_m)_{4\times4}$ corresponds to the covariance matrix of the two mechanical resonator modes, $(\Upsilon_o)_{4\times4}$ represents the covariance matrix of the two optical modes, and $(\Upsilon_{mo})_{4\times4}$ stands for the covariance matrix characterizing the interaction between the mechanical resonator mode and the optical mode cavity.[54,59] These matrices serve as essential tools for addressing the primary objective of this study, which is the examination of quantum entanglement and quantum correlations that extend beyond entanglement, originating exclusively between the two mechanical resonator modes. Consequently, our attention is directed toward the first block covariance matrix, describing the dynamics of the two vibrating mode, and is expressed as

$$(\Upsilon_{m_1m_2})_{4\times4}=\begin{pmatrix}\Upsilon_{m_1}&\Upsilon_{m_{12}}\\\Upsilon^{\rm T}_{m_{12}}&\Upsilon_{m_2}\end{pmatrix}, \quad (27)$$

where $(\Upsilon_{m1})_{2\times2}$ and $(\Upsilon_{m2})_{2\times2}$ pertain to the individual characteristics of the first and second mechanical modes, respectively. Meanwhile, $(\Upsilon_{m12})_{2\times2}$ delineates the interaction between the two mechanical resonator modes, reflecting the inter-mode correlations. By extracting the relevant components from the global covariance matrix outlined in Eq. (26),

we can establish the structure of $(\Upsilon_m)_{4\times4}$ as follows:

$$\Upsilon_{m_1m_2}=\begin{pmatrix}\Upsilon_1 & \Upsilon_2 & \Upsilon_3 & 0\\ \Upsilon_2 & \Upsilon_1 & 0 & -\Upsilon_3\\ \Upsilon_3 & 0 & \Upsilon_1 & \Upsilon_2\\ 0 & -\Upsilon_3 & \Upsilon_2 & \Upsilon_1\end{pmatrix}, \tag{28}$$

where $(\Upsilon_{m1})_{2\times2}$, $(\Upsilon_{m2})_{2\times2}$, and $(\Upsilon_{m12})_{2\times2}$ are defined as

$$\Upsilon_{m_1}=\Upsilon_{m_2}=\begin{pmatrix}\Upsilon_1 & \Upsilon_2\\ \Upsilon_2 & \Upsilon_1\end{pmatrix},\ \Upsilon_{m_{12}}=\begin{pmatrix}\Upsilon_3 & 0\\ 0 & -\Upsilon_3\end{pmatrix},$$

with their elements represented by Υ_1, Υ_2 and Υ_3,

$$\Upsilon_1=\Big[(-4\xi^2-(\kappa+\gamma)(\kappa+\gamma+\mathcal{C}\gamma))(2n_{\rm th}+1)-\cosh(2r)(\kappa+\gamma)\mathcal{C}\kappa\Big]\cdot\Big[2(4\xi^2+2(1+\mathcal{C})(\kappa+\gamma)^2)\Big]^{-1}, \tag{29}$$

$$\Upsilon_2=\frac{((2+\mathcal{C})\kappa+\gamma)\mathcal{C}\kappa^2\xi\sinh(2r)}{((1+\mathcal{C})^2\kappa^2+4\xi^2)((\kappa+\gamma)^2+4\xi^2)}, \tag{30}$$

$$\Upsilon_3=-\frac{((\mathcal{C}+1)\kappa(\gamma+\kappa)-4\xi^2)\mathcal{C}\kappa^2\sinh(2r)}{2(4\xi^2+(1+\mathcal{C})^2\kappa^2)(4\xi^2+(\kappa+\gamma)^2)}. \tag{31}$$

Here, Υ_1, Υ_2, and Υ_3 are dependent on various parameters, including the squeezing parameter r, the optomechanical cooperativity $\mathcal{C}$,[44] the mean thermal phonon number $n_{\rm th}$, the coupling strength ξ, and the damping rates γ and κ.

3. Quantification of quantum correlations

3.1. Analysis of entanglement via the logarithmic negativity

The first generalization in the quantification of entanglement in mixed states is certainly the logarithmic negativity.[60,61] This measure, known as $E^{\rm m}_{\mathcal{N}}$, is a powerful tool for characterizing entanglement within quantum systems. $E^{\rm m}_{\mathcal{N}}$ extends the entanglement quantifies to assess entanglement beyond pure states, making it suitable for the analysis of mixed quantum states. Unlike traditional entanglement measures that are tailored for pure states, the logarithmic negativity can be applied to a wider range of scenarios, where quantum systems are subjected to environmental interactions or exhibit complex statistical mixtures.

For a thorough examination of the system's entanglement properties, we turn our attention to the continuous-variable bipartite subsystem constituted by mirror (M_1) and mirror (M_2). Our primary aim is to explore the entanglement between these two movable mirrors, with a focus on the $E^{\rm m}_{\mathcal{N}}$. This measure is invaluable in quantifying the degree of entanglement and unveiling nonclassical correlations that exist within the subsystem. By applying the concept of logarithmic negativity, we can gain a deeper understanding of the complex quantum interactions that underlie the dynamics of the system, even in scenarios involving mixed states and intricate environmental influences. The global covariance matrix provided in Eq. (26) can be readily simplified to

$$(\Upsilon_{m_1m_2})_{4\times4}=\begin{pmatrix}\Upsilon_{m_1} & \Upsilon_{m_{12}}\\ \Upsilon^{\rm T}_{m_{12}} & \Upsilon_{m_2}\end{pmatrix}, \tag{32}$$

where $(\Upsilon_{m1})_{2\times2}$ and $(\Upsilon_{m2})_{2\times2}$ represent the covariance matrices of individual modes, and $(\Upsilon_{m12})_{2\times2}$ is the covariance matrix that characterizes the correlations between the two subsystems involving the movable mirrors, the logarithmic negativity[60,61] $E^{\rm m}_{\mathcal{N}}$ is defined as

$$E^{\rm m}_{\mathcal{N}}=\max[0,-\ln(2\mu^-)], \tag{33}$$

the entanglement between the two mechanical modes is quantified by the smallest symplectic eigenvalue, denoted as μ^-. This value is defined as

$$\mu^-=\sqrt{\frac{\Phi-\sqrt{\Phi^2-4\det\Upsilon_m}}{2}}, \tag{34}$$

here Φ is expressed as a function of the elements of the simplified covariance matrix [Eq. (27)] denoted by $\Phi=\det\Upsilon_{m_1}+\det\Upsilon_{m_2}-2\det\Upsilon_{m_{12}}$.

Equation (33) indicates that the entanglement between the two mechanical modes is established when $E^{\rm m}_{\mathcal{N}}>0$, which corresponds to the condition $\mu^-<1/2$.

3.2. Gaussian interferometric power

The concept of interferometric power for a bipartite quantum state serves as a valuable tool in quantifying the precision of parameter estimation within the realm of quantum metrology, see, for instance, Ref. [62]. This measure has been introduced to assess the accuracy of estimating parameters in the framework of quantum metrology and has found applications in various areas, such as quantum information and quantum communication. In the context of finite-dimensional systems, the interferometric power proves to be a reliable indicator of quantum correlations present in bipartite states, including those that are separable. It enables a quantitative assessment of the quantum correlations and the potential information that can be extracted from such states for enhanced precision in parameter estimation. Interferometric power, in essence, quantifies the usefulness of a quantum state for improving the precision of parameter estimation, particularly in the context of quantum metrology. It provides a measure of how quantum correlations can enhance the precision of parameter estimation and is relevant in various quantum information and communication tasks. In finite-dimensional systems, it can also detect quantum correlations in bipartite states, even when they are separable.[62,63]

For symmetric mixed two-mode Gaussian states $\rho_{\Upsilon_{m_1m_2}}$, the Gaussian interferometric power ($\mathcal{P}^{\rm m}_{\mathcal{G}}$) is defined as[62]

$$\mathcal{P}^{\rm m}_{\mathcal{G}}=\frac{I_m+\sqrt{I_m^2+J_mK_m}}{2J_m}, \tag{35}$$

where

$$I_m = (\det\Upsilon_{m_1} + \det\Upsilon_{m_{12}})(1 + \det\Upsilon_{m_1} + \det\Upsilon_{m_{12}} - \det\Upsilon_{m_1m_2}) - \Upsilon_{m_1m_2}^2, \tag{36}$$

$$J_m = (\det\Upsilon_{m_1m_2} - 1)(1 + 2\det\Upsilon_{m_1} + 2\det\Upsilon_{m_{12}} + \det\Upsilon_{m_1m_2}), \tag{37}$$

$$K_m = (\det\Upsilon_{m_1} + \Upsilon_{m_1m_2})((\det\Upsilon_{m_1m_2})^2 - \det\Upsilon_{m_1m_2}) + \det\Upsilon_{m_{12}}(2\det\Upsilon_{m_1} + \det\Upsilon_{m_{12}})(1 + \det\Upsilon_{m_1}). \tag{38}$$

By employing the covariance matrix, defined in Eq. (27), the expression for the Gaussian interferometric power ($\mathcal{P}_{\mathcal{G}}^{\mathrm{m}}$) as given in Eq. (35) can be re-equated as follows:

$$\mathcal{P}_{\mathcal{G}}^{\mathrm{m}} = \frac{\Upsilon_3^2}{2(\Upsilon_1^2 - \Upsilon_3^2 + 1/2)}, \tag{39}$$

where Υ_1 and Υ_3 are given by Eqs. (29) and (31).

4. Results and discussion

In this section, we give a comprehensive discussion of quantifying quantum correlations through two distinct metrics $E_{\mathcal{N}}^{\mathrm{m}}$ and $\mathcal{P}_{\mathcal{G}}^{\mathrm{m}}$. It was imperative to meticulously choose system parameters that accurately represent real-world scenarios feasible for experimental implementation. In this regard, we have adopted specific parameter values drawn from previous studies, such as those reported in Refs. [64,65]. These parameters have been tailored to closely mimic the conditions observed in recent experiments, thus ensuring the practicality and applicability of our analysis. To provide further insight into the system, the Fabry–Pérot cavities are characterized by specific parameter regimes, closely resembling those observed in recent experiments. Here are the specific parameter values: ($L_j \simeq 25$ mm, $m_j \simeq 145$ ng, $\omega_{mj}/2\pi = 947$ kHz, $\gamma_{mj}/2\pi \simeq 140$ Hz, $\kappa_j/2\pi \simeq 215 \times 10^3$ Hz, $T = 0.6$–20 K, $P = 11$ mW, $\xi = 10 \times 10^4$, $r = 3$, $\lambda_j = 1064$ nm).

Figure 2 provides a visual representation of how logarithmic negativity ($E_{\mathcal{N}}^{\mathrm{m}}$) and Gaussian interferometric power ($\mathcal{P}_{\mathcal{G}}^{\mathrm{m}}$) change with varying average numbers of thermal photons (n_{th}) across different cooperative parameter values. Both $E_{\mathcal{N}}^{\mathrm{m}}$ and $\mathcal{P}_{\mathcal{G}}^{\mathrm{m}}$ exhibit a similar response, as n_{th} increases, they decrease. This behavior can be explained by the influence of thermal photons on the system. Higher n_{th} values signify greater environmental fluctuations, leading to more significant losses of quantum information. As a result, both $E_{\mathcal{N}}^{\mathrm{m}}$ and $\mathcal{P}_{\mathcal{G}}^{\mathrm{m}}$ decrease, reflecting the challenge of maintaining quantum correlations in the presence of environmental noise. These findings emphasize the importance of carefully controlling thermal effects when working with such quantum systems.

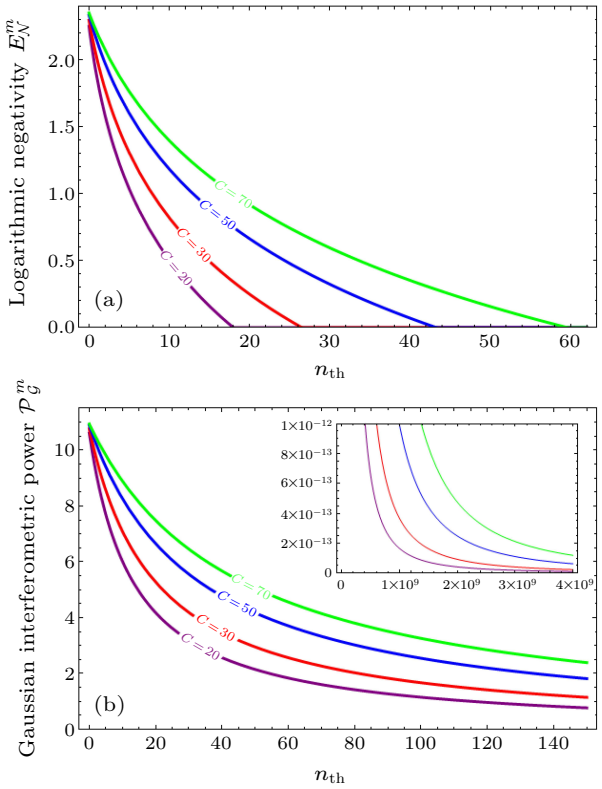


Fig. 2. The plot shows the amount of quantum correlations generated between two mechanical modes. (a) The behavior of logarithmic negativity $E_{\mathcal{N}}^{\mathrm{m}}$ is presented in terms of the average number of thermal phonons n_{th} for various values of the cooperative parameter $\mathcal{C}$. (b) The behavior of the Gaussian interferometric power $\mathcal{P}_{\mathcal{G}}^{\mathrm{m}}$ is depicted in terms of the average number of thermal phonons n_{th} for different values of the cooperative parameter $\mathcal{C}$.

In Fig. 3, we're examining how the logarithmic negativity ($E_{\mathcal{N}}^{\mathrm{m}}$) and Gaussian interferometric power ($\mathcal{P}_{\mathcal{G}}^{\mathrm{m}}$) respond to changes in the average number of thermal photons (n_{th}). These quantifiers are valuable tools for assessing quantum correlations between the two mechanical modes. The key result from this graph is that both $E_{\mathcal{N}}^{\mathrm{m}}$ and $\mathcal{P}_{\mathcal{G}}^{\mathrm{m}}$ exhibit similar trends. As we increase the cooperative parameter ($\mathcal{C}$), we observe a clear rise in the amount of quantum correlations generated between the two mechanical modes. This cooperative parameter reflects the strength of the photon hopping interactions within the system. However, the intriguing aspect is the difference in how these quantifiers behave in the presence of thermal noise. While both $E_{\mathcal{N}}^{\mathrm{m}}$ and $\mathcal{P}_{\mathcal{G}}^{\mathrm{m}}$ capture quantum correlations, $E_{\mathcal{N}}^{\mathrm{m}}$ is more susceptible to environmental influences. It declines rapidly with increasing thermal noise, ultimately approaching zero. On the other hand, $\mathcal{P}_{\mathcal{G}}^{\mathrm{m}}$ displays greater resilience against thermal noise, decreasing more gradually. This implies that $\mathcal{P}_{\mathcal{G}}^{\mathrm{m}}$ is a more robust indicator of quantum correlations under noisy conditions. Furthermore, it is important to note that $E_{\mathcal{N}}$ primarily detects quantum correlations related to entanglement, focusing exclusively on this form of quantum correlation. As a result, it might not capture quantum correlations that extend beyond entanglement. This limitation is where $\mathcal{P}_{\mathcal{G}}^{\mathrm{m}}$ shines. It has the capability to identify a

wider spectrum of quantum correlations, including those that are not entanglement-based. This is a valuable feature as it helps uncover quantum correlations of discord type and other non-entanglement quantum correlations, offering a more comprehensive view of the system's quantum behavior.

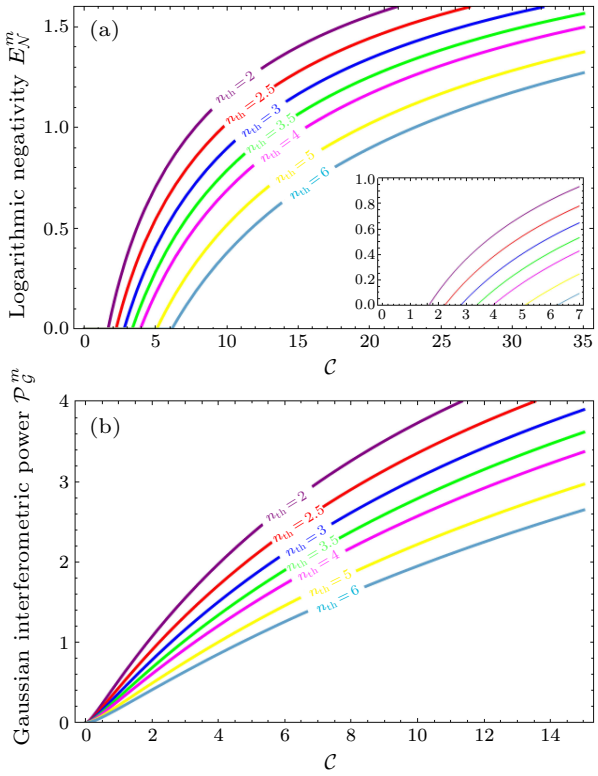


Fig. 3. The plot illustrates the amount of quantum entanglement as well as quantum correlations beyond entanglement generated between two mechanical modes. (a) The behavior of logarithmic negativity $E_{\mathcal{N}}^{\rm m}$ is displayed in terms of the cooperative parameter $\mathcal{C}$ for various values of the average number of thermal phonons $n_{\rm th}$. (b) Show cases the behavior of the Gaussian interferometric power $\mathcal{P}_{\mathcal{G}}^{\rm m}$ in terms of the cooperative parameter $\mathcal{C}$ for different values of the average number of thermal phonons $n_{\rm th}$.

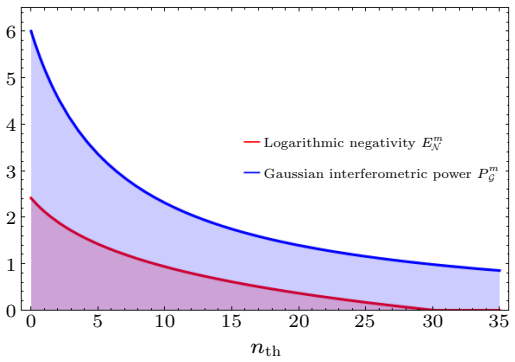


Fig. 4. Logarithmic negativity ($E_{\mathcal{N}}^{\rm m}$, depicted by the red line) and Gaussian interferometric power ($\mathcal{P}_{\mathcal{G}}^{\rm m}$, shown in blue) plotted against the thermal phonon number $n_{\rm th}$ for a squeezing parameter of $r = 1.5$ associated with the mechanical modes. In this analysis, we utilized a cooperative parameter $\mathcal{C} = 34$.

In Fig. 4, we observe that, with a fixed squeezing parameter r, both the logarithmic negativity ($E_{\mathcal{N}}^{\rm m}$) and the Gaussian interferometric power ($\mathcal{P}_{\mathcal{G}}^{\rm m}$) for the two mechanical modes decrease as the mean thermal phonon number $n_{\rm th}$ increases. This trend signifies that higher temperatures lead to the degradation of quantum features within the mechanical modes. Notably, the impact of thermal noise on mechanical entanglement, as represented by $E_{\mathcal{N}}^{\rm m}$, is much more severe as it rapidly diminishes to zero. Interestingly, $\mathcal{P}_{\mathcal{G}}^{\rm m}$ exhibits a different behavior. Beyond the entanglement threshold (i.e., when $E_{\mathcal{N}}^{\rm m} = 0$), $\mathcal{P}_{\mathcal{G}}^{\rm m}$ enters a frozen state, showing minimal sensitivity to temperature variations. In fact, it continues to persist and remains almost constant, reaching an asymptotic regime, even at elevated levels of mean thermal phonons (i.e., high temperatures).[66] This behavior highlights the robustness of $\mathcal{P}_{\mathcal{G}}^{\rm m}$ in the presence of thermal noise, making it a valuable indicator of quantum correlations in such conditions.

5. Conclusion

In conclusion, our study contributes to the investigation of entanglement, a prominent form of quantum correlation, within the vibrational modes of distinct mobile mirrors and spatially isolated mechanical nano-resonators via photon hopping. The proposed optomechanical system showcases the feasibility of generating quantum entanglement between the mechanical resonators by introducing photon-hopping interactions among the cavity modes. To quantify the quantum correlations produced by these mechanical modes, we harnessed two key metrics: the logarithmic negativity ($E_{\mathcal{N}}^{\rm m}$) and the Gaussian interferometric power ($\mathcal{P}_{\mathcal{G}}^{\rm m}$). Our comparative analysis shows clearly the superiority of $\mathcal{P}_{\mathcal{G}}^{\rm m}$ in capturing quantum correlations in contrast to $E_{\mathcal{N}}$, which is susceptible to environmental influences. Importantly, all the parameters considered in our study are experimentally viable, demonstrating the importance of preserving quantum correlations for quantum information processing and their potential use in various quantum tasks.

Notably, within optomechanical systems, the transference of quantum correlations between optical and mechanical modes holds paramount importance. Encoding information in the mechanical modes is widely recognized as a more effective means of entanglement preservation. Therefore, the practical implementation of this form of entanglement at the macroscopic level, specifically within mechanical resonators, can serve as a valuable resource for experimentally realizing a multitude of quantum protocols.

References

[1] Adesso G, Bromley T R and Cianciaruso M 2016 *J. Phys. A: Math. Theor.* **49** 473001
[2] Maziero J, Celeri L C, Serra R M and Vedral V 2009 *Phys. Rev. A* **80** 044102
[3] Bitbol M 1996 *Schrödinger's philosophy of quantum mechanics* **188** (Berlin: Springer)
[4] Adesso G 2007 arXiv:quant-ph/0702069
[5] Jones J A and Jaksch D 2012 *Quantum information, computation and communication* (Cambridge: Cambridge University Press)

[6] Paris M G 2009 *Int. J. Quantum Inform.* **7** 125
[7] Steane A M 1999 *Nature* **399** 124
[8] Ladd T D, Jelezko F, Laflamme R, Nakamura Y, Monroe C and O'Brien J L 2010 *nature* **464** 45
[9] Pellizzari T, Gardiner S A, Cirac J I and Zoller P 1995 *Phys. Rev. Lett.* **75** 3788
[10] Gisin N, Ribordy G, Tittel W and Zbinden H 2002 *Rev. Mod. Phys.* **74** 145
[11] Pirandola S, Andersen U L, Banchi L, Berta M, Bunandar D, Colbeck R and Wallden P 2020 *Adv. Opt. Photon.* **12** 1012
[12] Bennett C H, Brassard G and Ekert A K 1992 *Sci. Amer.* **267** 50
[13] Giovannetti V, Lloyd S and Maccone L 2011 *Nat. Photon.* **5** 222
[14] Giovannetti V, Lloyd S and Maccone L 2006 *Phys. Rev. Lett.* **96** 010401
[15] Lahlou Y, Bakmou L, Maroufi B and Daoud M 2022 *Quantum. Inf. Process.* **21** 248
[16] Kheirabady M S and Tavassoly M K 2023 *J. Phys. B: At. Mol. Opt. Phys.* **56** 035501
[17] Schrödinger E 1935 *Math. Proc. Cambridge Philos. Soc.* **31** 555
[18] Wu E *et al.* 2020 *Laser Phys.* **30** 065205
[19] Horodecki R, Horodecki P, Horodecki M and Horodecki K 2009 *Rev. Mod. Phys.* **81** 865
[20] Rafeie M, Tavassoly M K and Setodeh Kheirabady M 2022 *Ann. Phys.* **534** 2100455
[21] Sete E A, Svidzinsky A A, Eleuch H, Yang Z, Nevels R D and Scully M O 2010 *J. Mod. Opt.* **57** 1311
[22] Eleuch H 2010 *Int. J. Mod. Phys. B* **24** 5653
[23] Teufel J D, Donner T, Castellanos-Beltran M A, Harlow J W and Lehnert K W 2009 *Nat. Nanotechnol.* **4** 820
[24] Bruß D 2002 *J. Math. Phys.* **43** 4237
[25] Erhard M, Krenn M and Zeilinger A 2020 *Nat. Rev. Phys.* **2** 365
[26] Zyczkowski K, Horodecki P, Horodecki M and Horodecki R 2001 *Phys. Rev. A* **65** 012101
[27] Bennett C H, Brassard G, Cr'epeau C, Jozsa R, Peres A and Wootters W K 1993 *Phys. Rev. lett.* **70** 1895
[28] Danilishin S L and Khalili F Y 2012 *Living Rev. Relativ.* **15** 5
[29] Mancini S, Giovannetti V, Vitali D and Tombesi P 2002 *Phys. Rev. Lett.* **88** 120401
[30] Jost J D, Home J P, Amini J M, Hanneke D, Ozeri R, Langer C and Wineland D J 2009 *Nature* **459** 683
[31] Armour A D, Blencowe M P and Schwab K C 2002 *Phys. Rev. Lett.* **88** 148301
[32] Aspelmeyer M, Kippenberg T J and Marquardt F 2014 *Rev. Mod. Phys.* **86** 1391
[33] Rafeie M and Tavassoly M K 2023 *Eur. Phys. J. D* **77** 63
[34] Chen R X, Shen L T, Yang Z B, Wu H Z and Zheng S B 2014 *Phys. Rev. A* **89** 023843
[35] Vitali D, Gigan S, Ferreira A, Böhm H R, Tombesi P, Guerreiro A and Aspelmeyer M 2007 *Phys. Rev. Lett.* **9** 030405
[36] Liao C G, Xie H, Chen R X, Ye M Y and Lin X M 2020 *Phys. Rev. A* **101** 032120
[37] Blatt R and Wineland D 2008 *Nature* **453** 1008
[38] Joshi C, Larson J, Jonson M, Andersson E and Öhberg P 2012 *Phys. Rev. A* **85** 033805
[39] Chen R X, Liao C G and Lin X M 2017 *Sci. Rep.* **7** 14497
[40] Tian L 2013 *Phys. Rev. Lett.* **110** 233602
[41] Sete E A, Eleuch H and Ooi C R 2014 *J. Opt. Soc. Am. B* **31** 2821
[42] Lahlou Y, Maroufi B and Daoud M 2023 *Mod. Phys. Lett. A* 2350154
[43] Liao J Q, Wu Q Q and Nori F 2014 *Phys. Rev. A* **89** 014302
[44] Lahlou Y, Amazioug M, El Qars J, Habiballah N, Daoud M and Nassik M 2019 *Int. J. Mod. Phys. B* **33** 1950343
[45] Ludwig M, Safavi-Naeini A H, Painter O and Marquardt F 2012 *Phys. Rev. Lett.* **109** 063601
[46] Rastegarzadeh M, Tavassoly M K and Hassani Nadiki M 2023 *Quantum Inf. Process.* **22** 95
[47] Eftekhari F, Tavassoly M K and Behjat A 2022 *Physica A* **596** 127176
[48] Braginsky V B and Khalili F Y 1995 *Quantum measurement* (Cambridge: Cambridge University Press)
[49] Huang S and Agarwal G S 2009 *New J. Phys.* **11** 103044
[50] Giovannetti V and Vitali D 2001 *Phys. Rev. A* **63** 023812
[51] Sete E A, Eleuch H and Das S 2011 *Phys. Rev. A* **84** 053817
[52] Sete E A and Eleuch H 2012 *Phys. Rev. A* **85** 043824
[53] Mazzola L and Paternostro M 2011 *Phys. Rev. A* **83** 062335
[54] Lahlou Y, Maroufi B, El Qars J and Daoud M 2020 *J. Russ. Laser Res.* **41** 584
[55] Adesso G, Ragy S and Lee A R 2014 *Open Syst. Inf. Dyn.* **21** 1440001
[56] Braunstein S L and Van Loock P 2005 *Rev. Mod. Phys.* **77** 513
[57] Mari A and Eisert J 2009 *Phys. Rev. Lett.* **103** 213603
[58] Adesso G, Serafini A and Illuminati F 2004 *Phys. Rev. A* **70** 022318
[59] Den Dekker A J and Van den Bos A 1997 *J. Opt. Soc. Am. A* **14** 547
[60] Vidal G and Werner R F 2002 *Phys. Rev. A* **65** 032314
[61] Plenio M B 2005 *Phys. Rev. Lett.* **95** 090503
[62] Adesso G 2014 *Phys. Rev. A* **90** 022321
[63] Souza L A, Dhar H S, Bera M N, Liuzzo-Scorpo P and Adesso G 2015 *Phys. Rev. A* **92** 052122
[64] Gröblacher S, Hertzberg J B, Vanner M R, Cole G D, Gigan S, Schwab K C and Aspelmeyer M 2009 *Nat. Phys.* **5** 485
[65] Fainstein A, Lanzillotti-Kimura N D, Jusserand B and Perrin B 2013 *Phys. Rev. Lett.* **110** 037403
[66] Bromley T R, Cianciaruso M and Adesso G 2015 *Phys. Rev. Lett.* **114** 210401